BELLE2-NOTE-PL-2021-XXX
Draft version 1.0
March 25, 2021

Muon and electron identification efficiencies and hadron-lepton mis-identification rates at Belle II for Moriond 2021

Lepton ID Group, The Belle II Collaboration

Abstract

We present a collection of selected results on the performance of Belle II in the identification of electrons and muons. This work is based on a combination of sub-detector likelihoods and is carried out using data collected at the Belle II experiment from 2019 to mid-2020. These data correspond to a total integrated luminosity of $\int L\ \mathrm{dt} = 62.8\,\mathrm{fb}^{-1}$ collected at the center-of-mass energy of the $\Upsilon(4S)$ with an additional sample corresponding to $\int L\ \mathrm{dt} = 8.4\,\mathrm{fb}^{-1}$ of off-resonance data collected over the same period.

1. DATASET AND DEFINITIONS

The Belle II detector [1] is located around the interaction region of the asymmetric energy Super-KEKB electron-positron collider [2], at the KEK laboratory in Tsukuba, Japan. After a successful commissioning phase in 2018, the experiment has been collecting data at the center-of-mass (CM) energy of (or nearby) the $\Upsilon(4S)$ resonance since 2019. Electrons and positrons are accelerated at the Super-KEKB collider to energies of 7 GeV and 4 GeV, respectively, to boost the CM frame relative to the laboratory frame to $\beta\gamma = 0.28$.

In this document we present lepton identification (ID) studies ($\ell^\pm = \{e^\pm, \mu^\pm\}$) performed using the Moriond 2021 on-resonance datasets collected in 2019 (experiments 7, 8 and 10) amounting to 8.8 fb^{-1}, and 2020 (experiment 12) amounting to 54.0 fb^{-1}, as well as the 2020 off-resonance dataset for the D^{*+} channel (experiment 12) amounting to 8.4 fb^{-1}.

The Belle II detector is comprised of several sub-detector components arranged cylindrically around the interaction region. The vertex detector (VXD), the innermost detector element of Belle II, consists of two layers of silicon pixel detectors (PXD) and four layers of double-sided silicon strips detectors (SVD). In the data-taking period discussed in this document, only the innermost layer of the PXD was fully installed while, for the second layer, only two sensors were installed. However, the PXD and the SVD were not used for particle identification for the results shown here. The central drift chamber (CDC) is filled with a helium-based gas mixture for tracking charged particles and contributes to their identification via energy loss measurements (dE/dx). The time-of-propagation Cherenkov detector (TOP), consisting of 16 bars of fused silica, and the Aerogel Ring Imaging Cherenkov detector (ARICH), allow for the identification of charged hadrons. An electromagnetic calorimeter (ECL) consisting of 8,736 Thallium-doped CsI crystals distributed in a barrel and two endcaps (forward/backward) is used mainly for the identification of electrons/positrons and photons. Finally, the K_L^0 and muon detector (KLM) consists of a sandwich-like structure of alternating metal plates and active detector elements based on resistive plate chambers. A superconducting solenoid, situated between the ECL and the KLM, provides a 1.5 T axial magnetic field. A detailed description of the full detector is given in [1]. Information from each particle identification system $D = \{\text{CDC}, \text{TOP}, \text{ARICH}, \text{ECL}, \text{KLM}\}$ is analyzed independently to determine the likelihood of each charged particle hypothesis. These likelihoods may then be used to construct a combined likelihood ratio. A more detailed description of the Belle II lepton ID algorithms is given in Ref. [3].

In the results presented here, we study identification based on the global likelihood ratio, and from all contributing sub-detectors, defined as:

$$\ell\text{ID} = \frac{\mathcal{L}_\ell}{\mathcal{L}_e + \mathcal{L}_\mu + \mathcal{L}_\pi + \mathcal{L}_K + \mathcal{L}_p + \mathcal{L}_d}, \tag{1}$$

where:

$$\mathcal{L}_i = \prod_d^{d\in D} \mathcal{L}_i^d, \quad i \in \{e, \mu, \pi, K, p, d\} \tag{2}$$

We report the lepton identification performance of electron-hadron, and muon-hadron separation ($h^\pm = \{\pi^\pm, K^\pm\}$) using a complementary set of decay channels. Efficiency and mis-identification rate are defined as the probability for an electron (muon) track to be correctly identified as such, and the probability for a hadron track to be wrongly identified as a lepton track. Electron and muon identification efficiencies are studied using $e^+e^- \to$

$\ell^+\ell^-(\gamma)$, $e^+e^- \to e^+e^-\ell^+\ell^-$, and $J/\psi \to \ell^+\ell^-$, while pion mis-identification rates are studied using $K^0_S \to \pi^+\pi^-$, $e^+e^- \to \tau^\pm(1P)\tau^\mp(3P)$, and $D^{*+} \to D^0(\to K^-\pi^+)\pi^+$. The latter is also used to determine kaon mis-identification rates.

Other techniques for combining sub-detector data, such as boosted decision tree methods with a larger set of detector inputs, have also been developed for Belle II but are not yet used for physics analysis studies and therefore not covered here. Performance is evaluated in the polar angle acceptance regions corresponding to the electromagnetic calorimeter (ECL) for electrons (0.22 to 2.71 radians), and to the K^0_L-muon detector (KLM) for muons (0.40 to 2.60 radians). Combined, the set of probe channels covers a lab-frame momentum range of 0.4 GeV/c to 7.0 GeV/c for electrons and of 0.4 GeV/c to 6.5 GeV/c for muons. Results are also binned with respect to the track lab frame polar angle and measured track charge , although only results for an inclusive charge selection are shown here.

Lepton identification performance is studied for three reference selection thresholds on the ℓID variable: 0.5, 0.9 and 0.95. For brevity, the plots presented here show results for a selection of $\ell\text{ID} > 0.9$. The next sections provide an overview of the selected results obtained in the various studies. A general description of the selection criteria used to identify the final state is given in each section. Finally, in the last section we show the combination of all results assessing the lepton identification performance of Belle II in terms of efficiency and fake rates obtained in different acceptance regions and as a function of the momentum.

2. ANALYSES

2.1. Lepton identification efficiencies in $J/\psi \to \ell^+\ell^-$ decays

For the $J/\psi \to \ell^+\ell^-$ channel and all other channels described here, a tag and probe method is used to measure lepton identification efficiencies. In addition to event selection criteria, in this case we preselect hadronic events, tight selection criteria are applied to one lepton candidate, denoted the tag, leaving the other lepton unbiased, denoted the probe.

We reconstruct pairs of tracks with following criteria: the impact parameters must satisfy $|dr| < 2.0$ cm and $|dz| < 5.0$ cm, the track momenta must be $p_{\text{lab}} > 0.1$ GeV/c, and an ECL cluster is required to be matched to each track. Electron track momenta are corrected for bremsstrahlung. Furthermore we require tag tracks to satisfy eID > 0.95 (electron channel) or muID > 0.95 (muon channel). Finally a vertex fit is applied to the track pairs, where failed fits are rejected from further analysis. The di-lepton invariant mass distributions after all the above selection criteria, and additional probe criteria of eID > 0.95 (electron channel) or muID > 0.95 (muon channel) are shown in Fig. 1.

A binned maximum likelihood fit is used to determine the number of J/ψ candidates from the dilepton invariant mass, and ultimately the lepton identification efficiencies. The fit is then rerun to measure the efficiency of lepton identification criteria on the probe lepton. The fit is simultaneously performed both to candidates that pass the selection criteria and to those that fail. The efficiency is calculated from the "pass" and "fail" signal yields, N_{pass} and N_{fail} respectively, as

$$\epsilon = \frac{N_{\text{pass}}}{N_{\text{pass}} + N_{\text{fail}}}. \tag{3}$$

In the electron channel, the signal PDF is modelled with a Crystal Ball function summed with a bifurcated Gaussian and a Gaussian. In the muon channel, the signal is modelled with

a Gaussian function summed with a bifurcated Gaussian. A second-order polynomial is used to model the background for both channels. The model parameters for the signal PDFs are first determined in MC, which include the mean (common to each component), widths, tail parameters, and relative fractions of each component. In the fit to data, only a global mean and a width fudge factor are floated, with all other parameters fixed. This simultaneous fit uses the same signal shape in both the pass and fail samples. The systematic uncertainties in this analysis are primarily due to the fixed parameters in the fit PDFs. To determine the systematic uncertainty, each fixed parameter was varied by 1 σ of its nominal value based on the fits to MC.

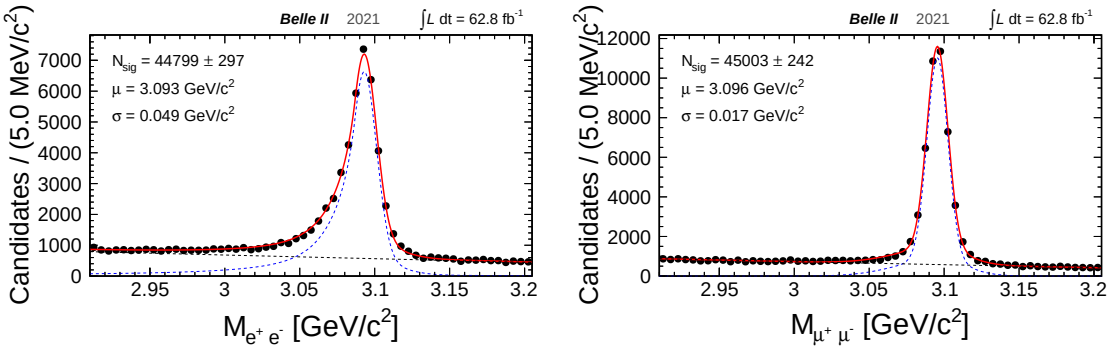

FIG. 1: The dielectron invariant mass of $J/\psi \to e^+e^-$ candidates (top), and dimuon invariant mass of $J/\psi \to \mu^+\mu^-$ candidates (bottom).

2.2. Lepton identification efficiencies in 2-photon events, $e^+e^- \to e^+e^-\ell^+\ell^-$

The selection criteria for each track in this channel are as follows: the impact parameters must satisfy $|dr| < 2.0$ cm, $|dz| < 5.0$ cm, and the track momenta required to be $p_{\rm lab} > 0.4$ GeV/c. The di-lepton invariant mass is required to be less than 3 GeV/c^2 and the event is required to have a visible energy in the CMS frame of $E_{vis} < 6$ GeV. In both cases, the dominant background is from the $e^+e^- \to e^+e^-\pi^+\pi^-$ process. The lepton ID efficiency is calculated through a tag and probe method. In the electron channel tight a electron identification requirement (eID > 0.95) is applied on the tag track e^+ (e^-) and the other track e^- (e^+) is used as a probe to determine the efficiency. For the muon identification efficiency, the tag side track is required to satisfy muID > 0.95 and $p > 0.7\,$GeV/c, where the latter requirement is needed to due to inefficient muon identification for low momentum tracks. A correction factor to account for hadron mis-identification is required to account for and correct background yields. The eID efficiency is defined as follows,

$$\epsilon = \frac{N_{\rm probe} - f \cdot \sum_T \sum_P n^{T,P}_{\rm probe} \cdot r_T \cdot r_P}{N_{\rm tag} - f \cdot \sum_T \sum_P n^{T,P}_{\rm tag} \cdot r_T} \tag{4}$$

where: $N_{\rm tag}$ and $N_{\rm probe}$ are the number of events after tag and probe selection, respectively; f is the fraction of events between data and MC before tag selections; $n_{\rm tag/probe}$ is the number of background events estimated in MC; r is the ratio of mis-identification probabilities in data to MC; and T and P indicate whether the track is tag or probe ($T,\ P = e, \mu, \pi, K, p$). Signal reconstruction plots are shown for $e^+e^- \to e^+e^-\ell^+\ell^-$ in Fig. 2.

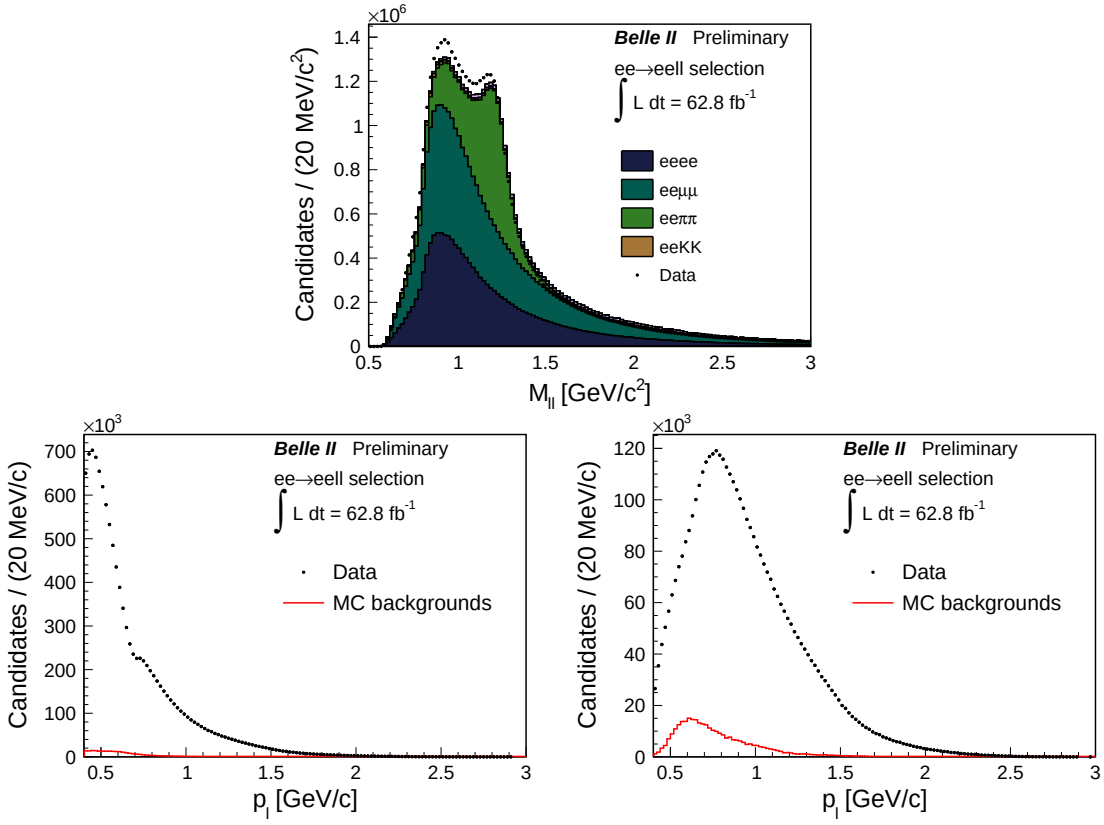

FIG. 2: Top row: the di-lepton invariant mass in $e^+e^- \to e^+e^-\ell^+\ell^-$ without tag particle identification criteria. Bottom row: the electron (left) and muon (right) lab-frame momentum distributions where a tag selection of $\ell ID > 0.95$ is applied. The red histogram shows the overall background contamination.

2.3. Muon identification efficiencies in radiative di-muon events, $e^+e^- \to \mu^+\mu^-\gamma$ events

Radiative di-muon signal events are selected requiring exactly two tracks originating from near the interaction point ($|dr| < 2.0$ cm and $|dz| < 5.0$ cm), and the radiated photon must have an energy E> 0.5 GeV with at least 1.5 hits per ECL cluster, and a polar angle acceptance of $-0.8660 < \cos\theta_{\rm lab} < 0.9563$ (within ECL acceptance). Muons are required to have momentum $0.7 < p_{\rm lab} < 8.0$ GeV/c. The total invariant mass of the $\mu^+\mu^-\gamma$ system is required to be $10.2 < M_{\mu^+\mu^-\gamma} < 10.8$ GeV/c^2. The muon used for tagging the event is required to have muID>0.9. Background from mis-identified pions is estimated to be less than 1% (0.3%) and originates predominantly from $e^+e^- \to \tau\tau$ ($\sigma = 0.919$ nb) and $e^+e^- \to \pi\pi\gamma$ ($\sigma = 0.167$ nb).

A tag and probe method is used for the muID efficiency estimation. Di-muon invariant mass, probe muon momentum, and tag muon polar angle distributions for the $e^+e^- \to \mu^+\mu^-\gamma$ process are shown in Fig. 3. The efficiency, $\epsilon^{data}_{\mu ID}$, is defined as follows:

$$\epsilon^{\rm data}_{\mu ID} = \frac{N_{\rm probe\ \mu} - \sum_i N^{\rm bkg,i,\mu}_{\rm probe} \cdot r^i_{\rm mis-id} \cdot r^{\mu}_{\rm mis-id}}{N_{\rm tag\ \mu} - \sum_i N^{\rm bkg,i}_{\rm tag} \cdot r^i_{\rm mis-id}} \quad \text{with} \quad i \in \{e, \pi, K, p, d\} \tag{5}$$

where $N_{\text{probe }\mu}$ ($N_{\text{tag }\mu}$) is the number of probe (tag) muons, $N^{\text{bkg},i,\mu}_{\text{probe}}$ is the number of probe MC background events per particle hypothesis i when the tag track is a muon, $N^{\text{bkg},i}_{\text{tag}}$ is the number of tag MC background events per particle hypothesis i, $r^{i}_{\text{mis-id}}$ is the ratio of mis-identification rates between data and MC. For the MC the efficiency $\epsilon^{MC}_{\mu ID}$ is evaluated as follows:

$$\epsilon^{\text{MC}}_{\mu\text{ID}} = \frac{N_{\text{probe }\mu}}{N_{\text{tag }\mu}} \tag{6}$$

The systematic error is only roughly estimated at present, varying $N^{\text{bkg}}_{\text{probe}}$ ($N^{\text{bkg}}_{\text{tag}}$) in Eq. 5 by 10%. The new efficiency value, calculated as in Eq. 5, is then subtracted to the original one and the absolute value of the difference is taken as the systematic attributed to the efficiency evaluation.

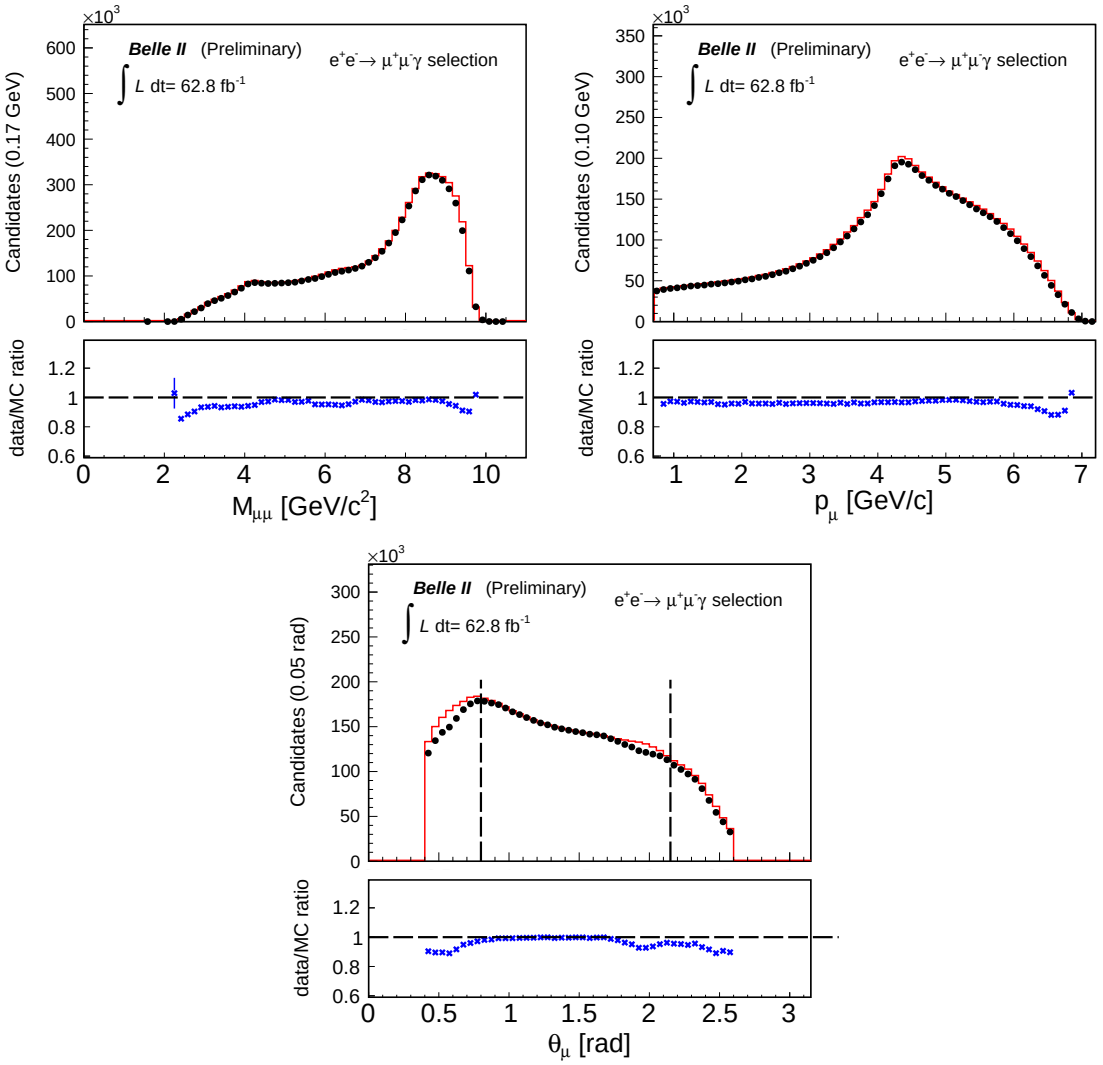

FIG. 3: The dimuon invariant mass (top), and muon lab-frame momentum (bottom) in $e^+e^- \to \mu^+\mu^-\gamma$.

2.4. Electron identification efficiencies in Bhabha scattering events, $e^+e^- \to e^+e^-(\gamma)$

Bhabha signal events are selected requiring exactly two tracks originating from near the interaction point ($|dr| < 2.0$ cm and $|dz| < 5.0$ cm). A criterion on the squared invariant mass of the system recoiling against the reconstructed e^+e^- pair of $M^2_{\text{recoil}} < 10\ \text{GeV}^2/c^4$ is applied to suppress hadronic background. The event must be triggered by an ECL cluster based low-multiplicity trigger (lml1) and the tag track is required to have an energy of at least $E > 2$ GeV in order to minimise trigger bias in the efficiency evaluation. The electron and positron track momenta after these selection criteria are applied are shown in Fig. 4.

The eID efficiency ϵ (Eq. 7) is calculated as the number of events, N_{probe}, satisfying the eID requirement placed on the probe, divided by the total number of selected events, N_{tag},

$$\epsilon = \frac{p_{\text{probe}} \cdot N_{\text{probe}}}{p_{\text{tag}} \cdot N_{\text{tag}}}. \tag{7}$$

Here $p_{\text{tag/probe}}$ denotes the probability that the probe electron (or the positron) candidate is correctly identified (i.e. a purity). These probabilities are computed using simulated $e^+e^- \to \{e^+e^-,\ e^+e^-\ell^+\ell^-,\ \mu^+\mu^-,\ \tau^+\tau^-\}$ samples as shown in Eq. 8

$$p_{\text{tag/probe}} = \frac{N^{\text{Sig}}_{\text{tag/probe}}}{N^{\text{BG}}_{\text{tag/probe}} + N^{\text{Sig}}_{\text{tag/probe}}}, \tag{8}$$

where $N^{\text{Sig}}_{\text{probe}}$ ($N^{\text{Sig}}_{\text{tag}}$) is the number of events with a correctly identified probe and $N^{\text{BG}}_{\text{probe}}$ ($N^{\text{BG}}_{\text{tag}}$) is the number of events with a mis-identified probe before (after) applying the electron ID requirement on the probe track. Two sources of systematic uncertainties are considered. To estimate possible bias introduced by the ECL trigger, the eID efficiency in the simulated Bhabha sample is evaluated by removing the trigger requirement, and the absolute difference between that and the result with the trigger requirement is taken as a systematic uncertainty. To estimate systematic effects due to background contamination, the eID efficiency in data is calculated with and without applying the purity factors, and the absolute difference is used as a source of systematic uncertainty. Systematic uncertainties are added in quadrature.

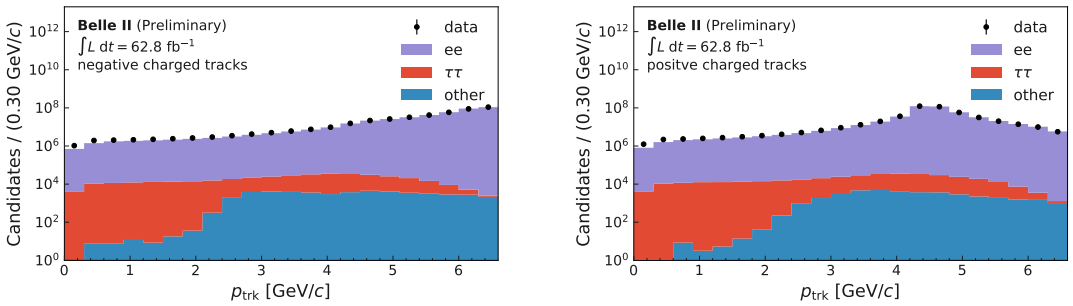

FIG. 4: The electron lab-frame momentum (left), and positron lab-frame momentum (right) in $e^+e^- \to e^+e^-(\gamma)$.

2.5. Pion mis-identification rates in $K^0_S \to \pi^+\pi^-$ decays

The K^0_S channel is used to measure the pion mis-identification rate in hadronic events. The selection criteria for tracks are as follows: $|dr| < 2.0$ cm, $|dz| < 5.0$ cm, $p_{\rm lab} > 0.1$ GeV/c and the matching ECL cluster energy must satisfy $E > 0.05$ GeV. A vertex fit is applied, selecting K^0_S candidates that do not fail the fit. The cosine of the angle between the K^0_S momentum vector and the decay vertex position vector is required to be $\cos(\theta(\vec{p}_{K^0_S}, \vec{V}_{K^0_S})) > 0.998$.

The mis-identification rate is measured by taking the ratio of the number of selected signal K^0_S candidates where at least one of the pion tracks passes a ℓID requirement ("pass") over the total number of K^0_S candidates ("pass+fail"). Similarly to the J/ψ analysis, the signal yields are extracted from a fit to the $M_{\pi^+\pi^-}$ distribution, which is shown in Fig. 5 without ℓID requirements, and with requirements on eID and muID to be greater than 0.95 on either of the pion tracks. A triple Gaussian is used to model the signal, and a first-order polynomial is used to model the background. The mass resolution is found to be approximately 5 MeV/c^2. For the systematic uncertainty evaluation, we follow the procedure used for $J/\psi \to \ell^+\ell^-$.

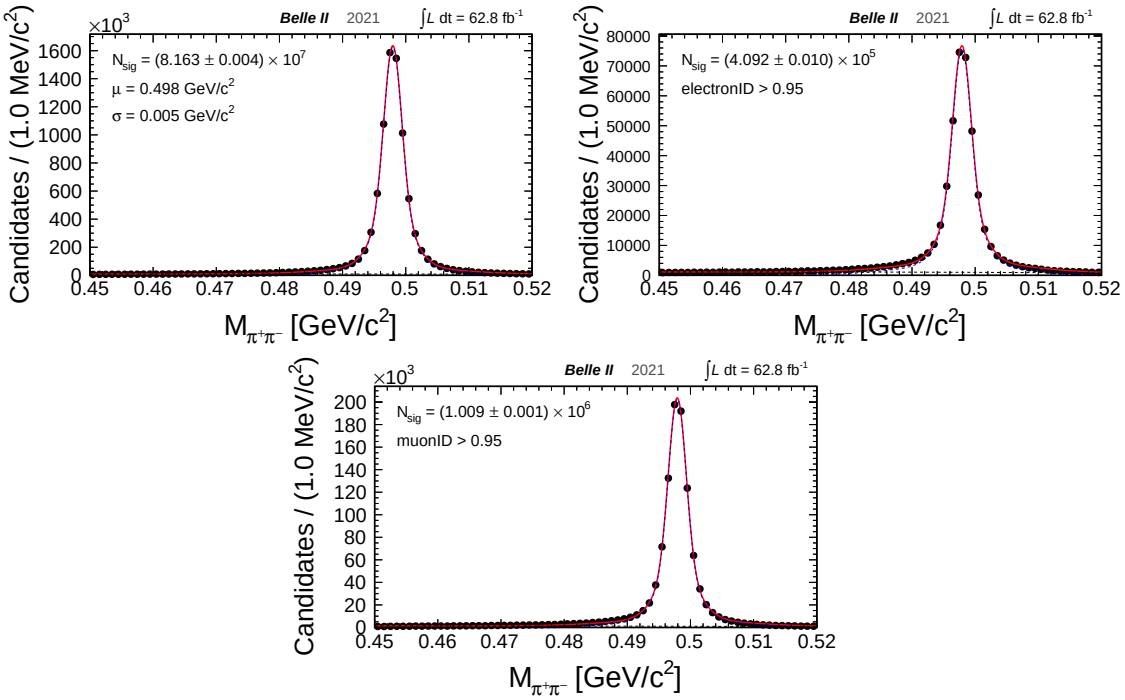

FIG. 5: The dipion invariant mass of $K^0_S \to \pi^+\pi^-$ before (top-left) and after application of eID > 0.95 (top-right) and muID > 0.95 (bottom) on one track in the pair.

2.6. Pion and kaon mis-identification rates in $D^{*+} \to D^0(K^-\pi^+)\pi^+$ decays

The D^{*+} channel is used to measure both the pion and kaon mis-identification rates in hadronic events. Each track is required to satisfy impact parameter criteria of $|dr| < 2.0$ cm and $|dz| < 4.0$ cm. The momentum of the D^{*+} in the CMS frame ($p_{D^{*+}}$) is required to be > 2.5 GeV/c to select prompt charm. A mass window on the $D^0 - D^{*+}$ invariant mass

difference $|\Delta M - 0.1453| < 1.5$ MeV/c^2 is required. Figure 6 shows the $K^-\pi^+$ invariant mass distributions with varying probe track criteria. We perform a binned maximumum likelihood fit to calculate the mis-identification rates in bins of track momentum, polar angle and charge. The signal is modeled with a double Gaussian distribution PDF sharing a common mean. Here, the mean is taken from the fit to the full dataset, and two Gaussian width terms are floated with a common fudge factor that accounts for varying resolution across each bin (similarly to the above resonance-based analyses). The background is modeled with a second-order Chebyshev polynomial PDF. The integrated luminosity of the dataset considered for this study corresponds to the combination of both on- and off-resonance data. Systematic effects in the fit are calculated varying the fixed PDF parameters, the mean and signal PDF fractions, within their statistical uncertainties, and varying the background PDF from first- to third-order the Chebyshev polynomials. Systematic effects in the latter are assessed as the difference between the two cases. All uncertainties are added in quadrature.

2.7. Pion mis-identification rates in $e^+e^- \to \tau^\pm(1P)\tau^\mp(3P)$ events

The selection criteria for each track on the 1P and 3P sides are as follows: $|dr| < 1.0$ cm, $|dz| < 3.0$ cm. The track on the 1P side is required to have $p_{\rm lab} > 0.1$ GeV/c. Three charged tracks are required to be in one hemisphere (3P-candidates) while only one is in the other (1P candidate). TreeFitter [4] is used to perform a vertex fit on the 3-prong side and a requirement on the $p-$value is employed to suppress combinatorial background. Signal reconstruction plots from mis-identification rate studies in $e^+e^- \to \tau^\pm(1P)\tau^\mp(3P)$ are shown in Fig. 7. In this study we used only a randomly selected fraction of it equivalent to 0.1×62.8 fb^{-1} to prevent from unblinding potential signals of interest with similar final states. The pion mis-identification rates, mis-ID($\pi \to \ell$), are calculated as:

$$\epsilon_{\rm data} = \frac{N_{\rm pid} - \sum_j n^j_{\rm pid} \cdot r_j}{N - \sum_j n^j} \quad \text{with} \quad j \in \{e, \mu, K, p, d\}, \tag{9}$$

where N is the total number of events remaining after all selections, $N_{\rm pid}$ is the number of events after applying an additional requirement on muID or eID, n^i and $n^i_{\rm pid}$ are the number of simulated background events per particle hypothesis i before and after the PID selection is applied, respectively, and r_i is the mis-ID rate ratio between data and MC. Systematic uncertainties in this procedure arise from uncertainties in the estimation of the n and r terms. Mismatches between simulated background and the background level in data is estimated by varying n based on the observed data/MC mismatch in the respective bin with the statistical error on the nominal value of n also propagated as a systematic error. Systematic errors due to trigger biases are estimated on data with the statistical uncertainty on the trigger correction also propagated as a systematic uncertainty to the final result. All uncertainties are then added in quadrature.

2.8. Results overview

We have evaluated efficiency and mis-identification rates as a function of track polar angle θ, lab frame momentum p and charge. We overlay efficiencies and mis-identification rates

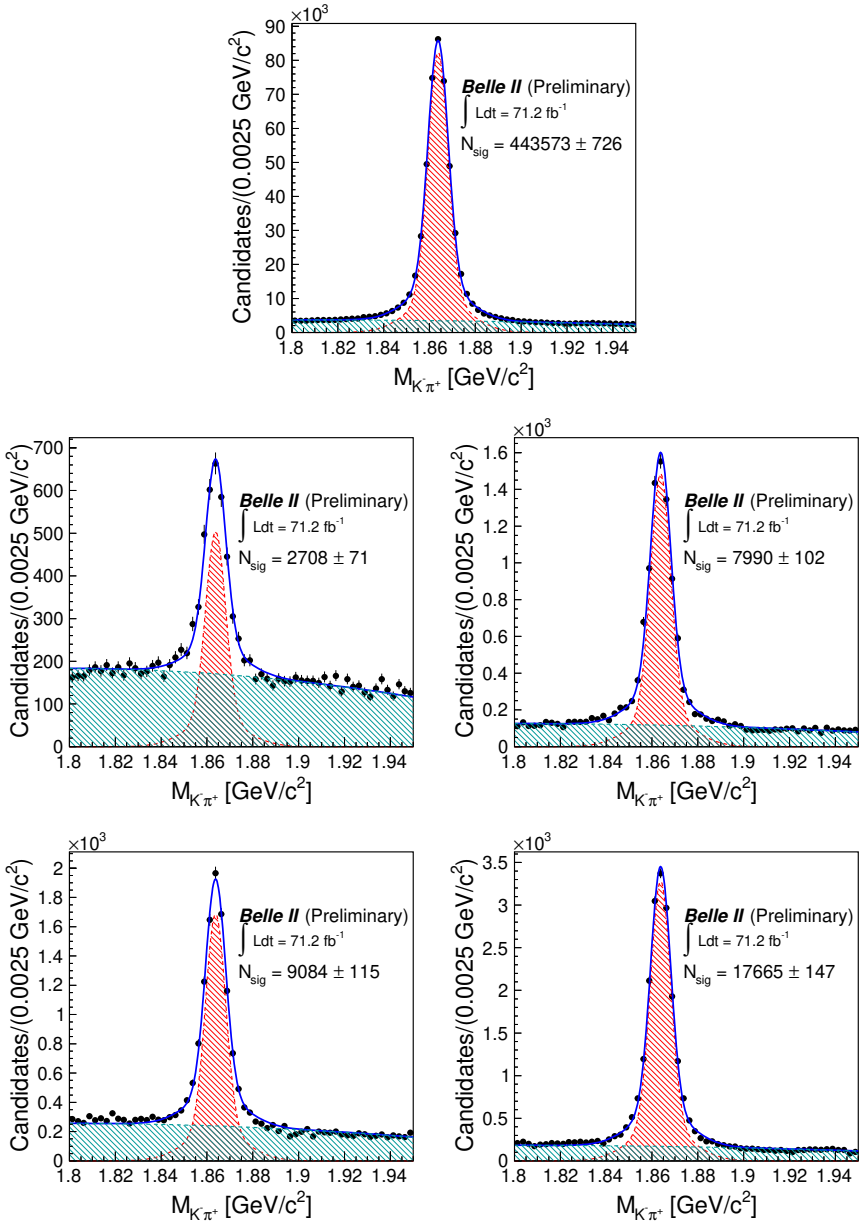

FIG. 6: $D^{*+} \to D^0(\to K^-\pi^+)\pi^+$ invariant mass plots without probe selection criteria (top), with eID>0.9 for the kaon track (middle left), with muID>0.9 for the kaon track (middle right), with eID>0.9 for the pion track (bottom left), and with muID>0.9 for the pion track (bottom right).

for all channels in two example barrel region polar angle bins for eID and muID, averaged over track charge, in Fig. 8. We also overlay the efficiency and mis-identification rates for two hadronic channels, J/ψ and K^0_S for eID > 0.9 integrated over the ECL barrel region (Fig. 9) and muID > 0.9 integrated over the KLM barrel region (Fig. 9). In such regions, the average lepton identification efficiency from these two hadronic channels is:

$$\epsilon(e) = 0.937 \pm 0.004 \text{ (stat.)} \pm 0.001 \text{ (syst.)} \tag{10}$$
$$\epsilon(\mu) = 0.868 \pm 0.004 \text{ (stat.)} \pm 0.001 \text{ (syst.)}, \tag{11}$$

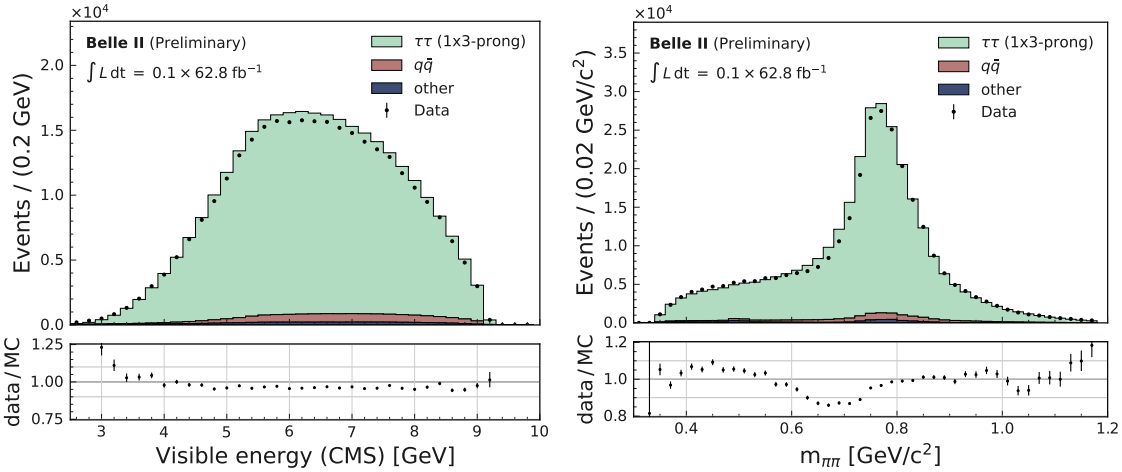

FIG. 7: The distributions of visible energy in the CMS and the invariant mass of the pion pairs in data and MC after background suppression.

for a pion mis-identification rate:

$$\text{mis} - \text{ID}(\pi \to e) = 0.022 \pm 0.009 \times 10^{-2}\ (\text{stat.}) \pm 0.006 \times 10^{-2}\ (\text{syst.}) \tag{12}$$

$$\text{mis} - \text{ID}(\pi \to \mu) = 0.072 \pm 0.008 \times 10^{-2}\ (\text{stat.}) \pm 0.006 \times 10^{-2}\ (\text{syst.}). \tag{13}$$

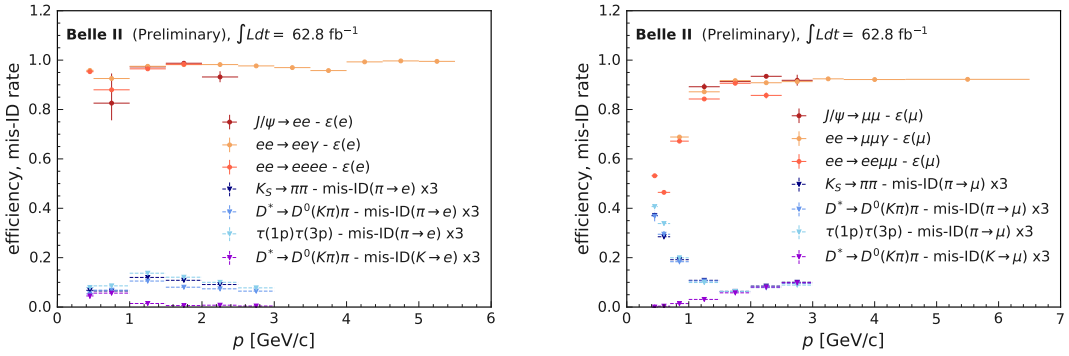

FIG. 8: Left: ECL barrel bin ($1.57 \leq \theta < 1.88$ rad) for eID > 0.9 with all measurements, efficiencies and hadron-lepton mis-identification rates overlaid. Note that the mis-identification rate has been multiplied by a factor of 3 for illustration purposes. Right: KLM barrel bin ($0.82 \leq \theta < 1.16$ rad) for muID > 0.9 with all measurements, efficiencies and hadron-lepton mis-identification rates overlaid. Note that the mis-identification rate has been multiplied by a factor of 3 for illustration purposes.

A combination of the ratios of efficiencies and mis-identification rates between data and MC in each bin from all channels is done following the procedure outlined in Ref. [5], approximating the likelihoods of each measurement as Gaussian functions and under the following assumptions: the measurements are statistically independent; if more than two measurements can be combined in a specific bin, then the combination is done associatively;

systematic errors sources are independent; measurements are combined in a specific bin only if they are consistent within 1σ (where σ accounts for both statistical and systematic uncertainties).

The first condition is satisfied because each measurement applies its selection criteria, and these are different and independent of the others; consequently the phase-space regions selected are different. The independence of the systematic source is guaranteed by the fact that they are specific to the method used in each measurement and this is specific to the measurement. If two measurements to be combined in a bin are not consistent within 1σ, we assign an extra systematic uncertainty as the "distance" between the central value of the combination to the minimum (maximum) central values among individual methods in each bin. We consider this residual discrepancy between channels to be caused predominantly by different levels of activity in the detector from nearby tracks and clusters around particle candidates selected in hadronic events - such as in J/ψ, K^0_S, D^* decays - as opposed to candidates from low multiplicity events. These effects will be thoroughly investigated. Results for the eID and muID efficiency ratios between data and simulation as a function of momentum for two selected bins in the ECL and KLM barrel, together with the combination of individual channels, are shown in Fig.10.

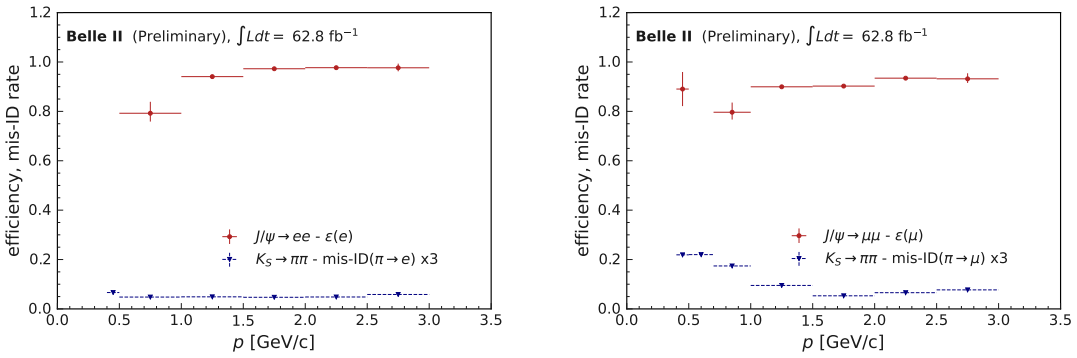

FIG. 9: Left: J/ψ and K^0_S efficiency and fake rate overlay for eID integrated over the entire ECL barrel region ($0.56 \leq \theta < 2.23$ rad), as a function of track momentum. Note that the hadron mis-identification rate has been inflated by a factor 3 for illustration purposes. Right: J/ψ and K^0_S efficiency and mis-identification rate overlay for muID integrated over the entire KLM barrel region ($0.82 \leq \theta < 2.13$ rad), as a function of track momentum. Note that the hadron mis-identification rate has been inflated by a factor 3 for illustration purposes.

2.9. Conclusion

We have presented the status of lepton identification efficiencies and hadron mis-identification rates at Belle II based on a likelihood classifier method. A broad set of calibration channels in different event topologies have been analysed. We find the performance in barrel region benchmark studies of lepton identification efficiencies with $J/\psi \to \ell\ell$ to be $\epsilon(e) = 0.937 \pm 0.004$ (stat.) ± 0.001 (syst.) for electrons with eID> 0.9, $\epsilon(\mu) = 0.868 \pm 0.004$ (stat.) ± 0.001 (syst.) for muons with muID> 0.9, corresponding to pion mis-identification rates with $K^0_S \to \pi^+\pi^-$ of $\text{mis} - \text{ID}(\pi \to e) = 0.022 \pm$

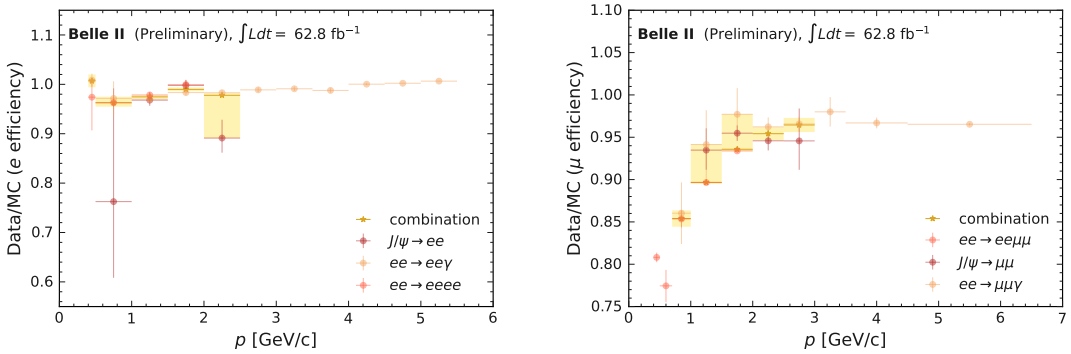

FIG. 10: Left: eID > 0.9 efficiency ratio between data and MC for individual channels and their combination in a selected ECL barrel bin ($1.57 \leq \theta < 1.88$ rad), as a function of track momentum. Right: muID > 0.9 efficiency ratio between data and MC for individual channels and their combination in a selected KLM barrel bin ($0.82 \leq \theta < 1.16$ rad), as a function of track momentum. The orange shaded band represents the total statistical plus systematic uncertainty on the combined result.

0.009×10^{-2} (stat.) $\pm\, 0.006 \times 10^{-2}$ (syst.) for electron candidates, and $\text{mis} - \text{ID}(\pi \to \mu) = 0.072 \pm 0.008 \times 10^{-2}$ (stat.) $\pm\, 0.006 \times 10^{-2}$ (syst.) for muon candidates. A set of upgrades to the baseline likelihood methods is in preparation.

[1] T. Abe (Belle II Collaboration) (2010), arXiv:1011.0352.
[2] Y. Ohnishi, T. Abe, T. Adachi, K. Akai, Y. Arimoto, K. Ebihara, K. Egawa, J. Flanagan, H. Fukuma, Y. Funakoshi, et al., Progress of Theoretical and Experimental Physics **2013** (2013), ISSN 2050-3911, URL `https://doi.org/10.1093/ptep/pts083`.
[3] E. Kou, P. Urquijo, et al. (Belle-II), PTEP **2019**, 123C01 (2019), [Erratum: PTEP 2020, 029201 (2020)], arXiv:1808.10567.
[4] J. F. Krohn et al. (Belle-II analysis software Group), Nucl. Instrum. Meth. A **976**, 164269 (2020), arXiv:1901.11198.
[5] R. Barlow, in *Statistical Problems in Particle Physics, Astrophysics and Cosmology* (2004), physics/0406120.